# Structural insight into the role of the ribosomal tunnel in cellular regulation

Rita Berisio[1,2], Frank Schluenzen[1], Joerg Harms[1], Anat Bashan[3], Tamar Auerbach[3,4], David Baram[3] and Ada Yonath[1,3]

Published online 31 March 2003; doi:10.1038/nsb915

**Nascent proteins emerge out of ribosomes through an exit tunnel, which was assumed to be a firmly built passive path. Recent biochemical results, however, indicate that the tunnel plays an active role in sequence-specific gating of nascent chains and in responding to cellular signals. Consistently, modulation of the tunnel shape, caused by the binding of the semi-synthetic macrolide troleandomycin to the large ribosomal subunit from *Deinococcus radiodurans*, was revealed crystallographically. The results provide insights into the tunnel dynamics at high resolution. Here we show that, in addition to the typical steric blockage of the ribosomal tunnel by macrolides, troleandomycin induces a conformational rearrangement in a wall constituent, protein L22, flipping the tip of its highly conserved β-hairpin across the tunnel. On the basis of mutations that alleviate elongation arrest, the tunnel motion could be correlated with sequence discrimination and gating, suggesting that specific arrest motifs within nascent chain sequences may induce a similar gating mechanism.**



In ribosomes, the site of peptide bond formation, called the peptidyl transferase center, is adjacent to the entrance of a tunnel along which nascent proteins progress until they emerge out of the ribosome. This exit tunnel, first observed in the mid-1980s[1,2], was assumed to provide a passive path that does not interact with the exported proteins and is not involved in their progression. Alterations of the exit tunnel diameter, correlated with mutations and different functional states, suggested that this tunnel may possess dynamic properties[3]. Recent evidence for the participation of the tunnel in regulating intracellular co-translational processes indicated that the tunnel may function as a discriminating gate, as it responds to specific sequence motifs of nascent chains that can affect protein elongation[4,5]. Striking examples of such effects are the SecM (secretion monitor) protein, which monitors protein export[6,7], and the nascent leader peptide of *Escherichia coli* tryptophanase (tnaC) operon[8].

The SecM protein includes a sequence motif that causes translation arrest in the absence of a protein export system (called also 'pulling protein'), which recognizes an export signal located at the N terminus of SecM[7–9]. The elongation arrest can be bypassed by mutations in the rRNA or in ribosomal protein L22 (ref. 7), a constituent of the ribosomal exit tunnel wall[10,11]. The L22 protein consists of a single globular domain and a highly conserved β-hairpin with a unique twisted conformation. This β-hairpin maintains its length in all species, whereas insertions and deletions exist in other regions of L22. Within the ribosome, the L22 protein is positioned with its globular domain on the surface of the large subunit and its β-hairpin extends ~30 Å away from the protein core[10,11]. The overall conformation of L22 in the ribosome is similar to that seen in the crystal structure of the isolated protein[12], except for a small difference in the inclination of the tip of its β-hairpin.

Macrolide antibiotics were shown to interfere with protein biosynthesis by blocking the exit tunnel[13–15]. Troleandomycin (TAO) belongs to the group of macrolides that, in addition to hampering protein biosynthesis, are prone to form nitrosoalkanes and consequently inactivate the liver cytochrome P450–metabolite complexes. Among the macrolides, TAO ranked first in causing a significant decrease of metabolism and may lead to cholestatic jaundice or hepatitis[16]; therefore, it is used as an antibiotic drug only in extreme cases. TAO is a semi-synthetic macrolide that shares structural features with the clinically relevant and commonly used 14-member macrolides, such as erythromycin or roxithromycin. It is built of a lactone ring and two sugar moieties, desosamine and cladinose. In comparison to erythromycin, TAO has an oxirane ring that replaces a methyl at position C9 of the lactone ring and lacks five hydroxyl groups, three of which are replaced by acetyl groups[17] (Fig. 1*a*). The unique chemical structure of TAO and the discovery of pentapeptides conferring resistance to oleandomycin[18,19], its predecessor compound, prompted us to investigate its binding mode and its inhibitory mechanism.

To analyze the action and the binding mode of TAO, we determined the crystal structure of the large ribosomal subunit from *Deinococcus radiodurans* (D50S) in complex with TAO at 3.4 Å resolution (Table 1). Analysis of the electron density maps (Fig. 1) allowed the unambiguous definition of the TAO-binding site and showed a different conformation of the highly conserved β-hairpin of the protein L22 that is induced by TAO binding. These results explain the inhibitory action of TAO. Furthermore, the striking conformational differences induced by TAO binding to the narrowest region of the ribosomal tunnel may provide structural clues for possible roles for the tunnel in regulating intracellular events.

## An unusual mode of macrolide binding

Similar to macrolides and azalides[13–15], TAO binds to the large ribosomal subunit near the tunnel entrance (Fig. 1*b*). It is, however, located deeper in the tunnel and, instead of being nearly

[1]Max-Planck-Research Unit for Ribosomal Structure, Hamburg, Germany. [2]Permanent address: Institute of Biostructure and Bioimaging, CNR, Napoli, Italy. [3]Department of Structural Biology, Weizmann Institute of Science, Rehovot, Israel. [4]Institute of Biochemistry, the Free University, Berlin, Germany.

Correspondence should be addressed to A.Y. *e-mail: ada.yonath@weizmann.ac.il*

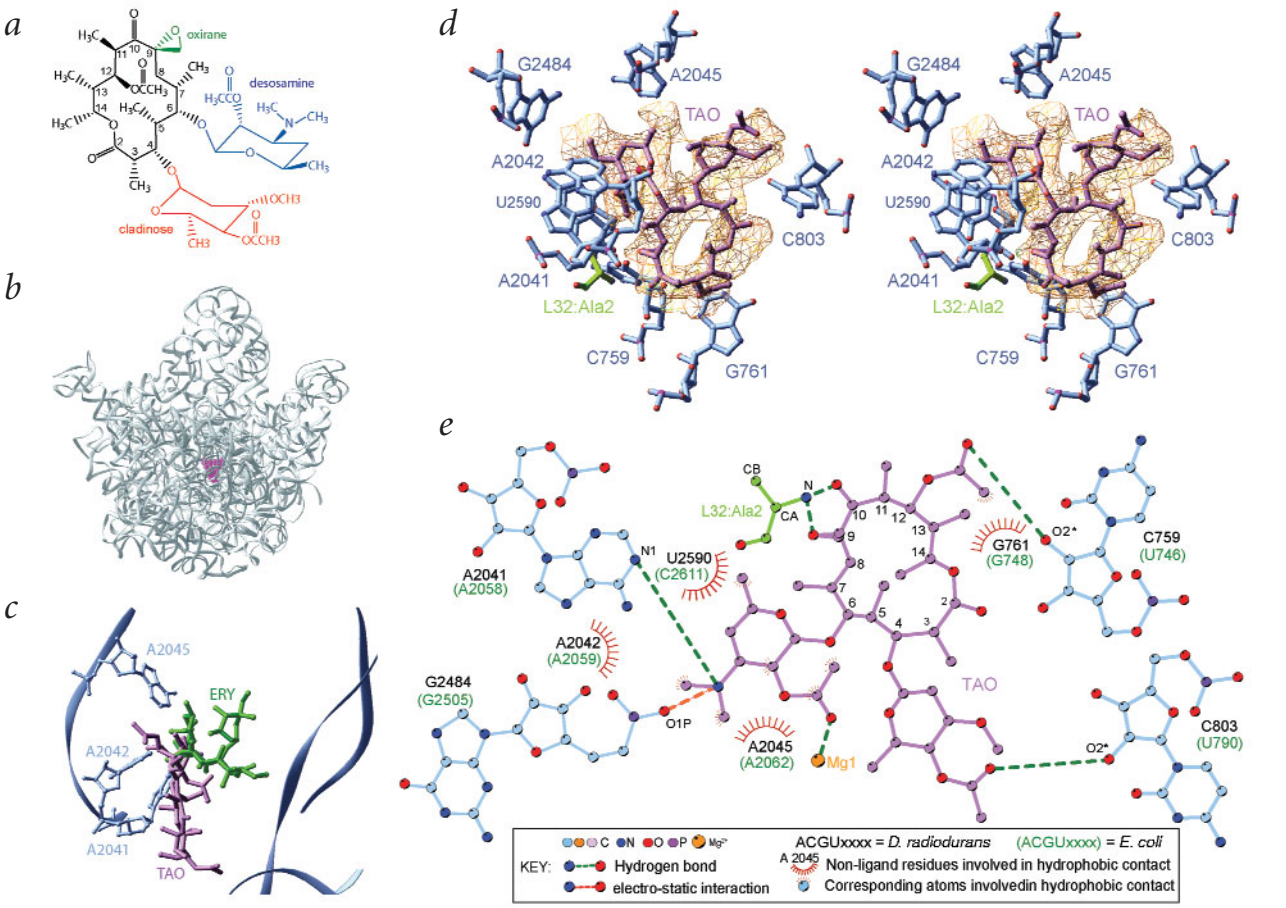


**Fig. 1** The binding mode of TAO to the large ribosomal subunit. ***a***, TAO chemical structure. ***b***, Interface view of the large ribosomal subunit (D50S) showing the location of bound TAO (magenta). D50S is represented by gray ribbons showing its RNA trace. ***c***, Superposition of TAO (pink) and erythromycin (ERY, green) bound within the tunnel of D50S (blue). The bases of the three nucleotides common to TAO and erythromycin interactions with the ribosome are shown. ***d***, Stereo view showing the omit electron density of TAO (pink) and its binding site in D50S. ***e***, A schematic showing TAO interactions with the large ribosomal subunit. Colors are as in (*d*).

perpendicular to the tunnel wall as observed for erythromycin and azithromycin[13,15], the TAO lactone ring forms a 20° angle with the tunnel wall (Fig. 1*c*) with its center of mass located 7 Å and 6 Å away from those of erythromycin and azithromycin, respectively.

Common to TAO and erythromycin are the interactions of the desosamine sugars with adenine A2041DR (A2058EC) (nucleotides and amino acids are numbered according to *D. radiodurans* (DR) followed by the *E. coli* (EC) numbers in parentheses). A2058EC was implicated in macrolide resistance and selectivity *via* mechanisms based on modifications of its base, either by di-methylation by Erm methylases or by mutation to guanine[20], the nucleotide commonly found in eukaryotes and archaea at this position (reviewed in ref. 21). Unique to TAO are the interactions of its lactone ring with protein L32 and with the hairpin of H35, as well as of its cladinose sugar with H35a (Fig. 1*d*,*e*), two helical features in domain II of the 23S RNA of the large ribosomal subunit. The TAO interactions seen in the crystal structure of its complex with D50S are consistent with RNA probing results, showing that in addition to the common interactions of macrolides with the vicinity of A2058EC, TAO binding protects the vicinity of domain II nucleotides 759–761DR (746–748EC) of H35, and 803–804DR(790–791EC) of H35a (T.A., D.B. and A.Y., to be published). These interactions are also in accord with the cross-resistance between mutants, induced in *D. radiodurans*, which show resistance to TAO and to the ketolide ABT-773 (T.A., D.B. and A.Y., to be published), because it was suggested[20,22,23] and confirmed at high resolution[15] that ketolides interact with domain II.

We presume that the specific binding mode of TAO is due mainly to its inability to interact with the tunnel in a manner similar to that of the common macrolides. Previous studies have shown that the desosamine hydroxyl group has a critical role in erythromycin binding[24]. Consistently, TAO was shown to serve as the anchoring feature of various macrolides, azalides and ketolides[13–14]. By superposition of TAO structure on those of erythromycin and azithromycin, we verified that the presence of an acetyl moiety on TAO desosamine sugar disables the formation of hydrogen bonds. Furthermore, TAO cannot bind similarly to these other macrolides, because an acetyl group instead of the typical macrolide desosamine hydroxyl group introduces steric hindrance in the neighborhood of A2041DR (A2058EC). The difference between the TAO binding mode to D50S and that of azithromycin to *Haloarcula marismortui* 50S (H50S)[14] may also be ascribed to the substitution of the key nucleotide for macrolide binding, selectivity and resistance, A2058EC, to guanine in H50S. A2058 is one of the few nucleotides of the peptidyl transferase ring that are not conserved among all phylogenetic domains, and sequence comparisons show that this nucleotide is almost always an adenine in

prokaryotes, whereas archaea and higher eukaryotes have a guanine at this position[24].

## Striking rearrangements in the exit tunnel

In the complex of D50S with TAO, the conformation of the tip of the β-hairpin of L22 differs significantly from that observed in the native structure of D50S (Fig. 2). This region contains a highly conserved arginine, Arg109DR (Arg88EC), a moderately conserved arginine or lysine, namely Arg111DR (Lys90EC), and an invariant alanine, Ala110DR (Ala91EC). Superposition of the location of TAO on native D50S structure revealed that its lactone-ring acetyl occupies the space originally occupied by Arg111DR (Fig. 2*c*). In the native D50S structure, the side chain of Arg111DR is embedded in a narrow groove formed by nucleotides C759–A762DR (U746–A749EC) and A764DR (A751EC) that limits the space available for conformational rearrangements of Arg111DR. Consequently, the binding of TAO triggers a substantial conformational rearrangement in the tip of L22 β-hairpin that is flipped around two hinges (built of residues 105–107DR (84–86EC) and 113–115DR (92–94EC)), across the tunnel. Upon this conformational rearrangement, the backbone of Arg111DR is shifted by ~13 Å (Fig. 2).

Both the native and the altered conformation of L22 β-hairpin (called here the 'swung conformation') are stabilized mainly by electrostatic interactions and hydrogen bonds with the backbone of rRNA. In the native conformation, Arg109DR interacts with backbone of G761DR (748EC), whereas Arg111DR lines the tunnel wall. In the swung conformation, Arg109DR interacts with the backbone of C1270DR (C1257EC) and C1271DR (U1258EC), while Arg111DR forms electrostatic interactions with C809DR (C796EC) (Fig. 2*c*). These two arginines (or the arginine and the lysine) may be considered as a 'double hook' that anchors both native and swung conformations and modulates the switch between them. The structure of protein L22 appears to be designed for its gating role. Precise positioning of L22 hairpin stem, required for accurate swinging and anchoring of the double-hook, is presumably achieved by the pronounced positive surface charges of this region[12].

## A proposed mechanism for tunnel gating

The observed swing of the tip of L22 β-hairpin indicates its intrinsic conformational mobility. As the swung conformation severely restricts the space available for the passage of nascent proteins through the tunnel and because the L22 double hook is highly conserved, it is tempting to link the swing of L22 with the putative regulatory role assigned to the tunnel. We propose that L22 is a main player is this task, with its double hook acting as a conformational switch and providing the molecular tool for the gating and the discriminative properties of the ribosome tunnel. Our proposal is based on the observation that sequence-related translational arrest could be suppressed by mutations[7] localized to the double-hook region of protein L22.

The motif FXXXXWIXXXXGIRAGP (where X is any amino acid) was shown to induce elongation arrest in *E. coli* while SecM protein is being synthesized. Within this sequence, the Pro, Trp and its adjacent Ile were identified to be the main features that trigger the arrest. This particular sequence motif was also found to hinder translation elongation in *E. coli* when

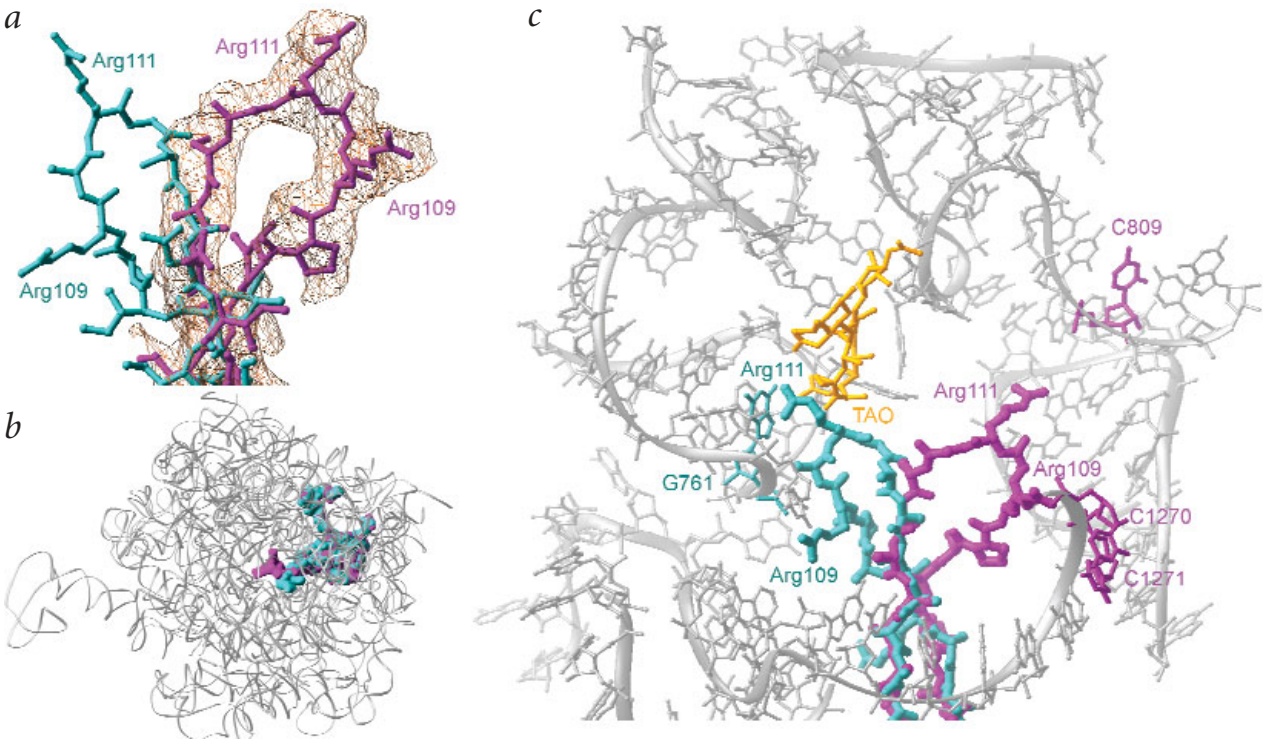


**Fig. 2** The global conformational changes of L22 hairpin triggered by TAO binding. ***a***, Omit electron density map for the swung conformation (magenta) of L22 β-hairpin. For comparison, the native conformation is also shown (cyan). The hinge region is at the bottom of the diagram. ***b***, View into the ribosomal tunnel from the active site, showing the hindrance of the tunnel by the swung conformation of L22 (magenta) compared with its native conformation (cyan). Note how the native and swung double-hooks interact with two sides of the tunnel wall. The large ribosomal subunit is represented by a gray ribbon trace of the rRNA. ***c***, Side view of the region of the ribosome exit tunnel, showing the contacts of the native (cyan) and swung (magenta) conformations of L22 hairpin tip. Note the collision between TAO (yellow) and the tip of L22 β-hairpin at its native conformation. The RNA moieties that form the tunnel wall at this region are shown in gray. The main interactions of the double hook arginines of the native and the swung conformations are indicated with their respective colors.

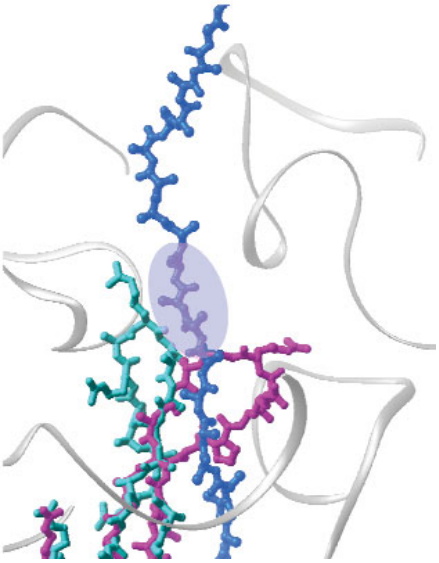

**Fig. 3** The putative progression of SecM arrest in the exit tunnel. The polyalanine chain (dark blue) is modeled together with the native (cyan) and the swung (magenta) L22 β-hairpin conformations. The region highlighted in purple corresponds to Trp155 and Ile156 in the *secM* sequence[7]. The wall of the ribosome exit tunnel is represented by the RNA backbone (gray).

present in the unrelated sequence of LacZα protein[7], indicating that the elongation arrest is independent of the sequence context around this motif. A feasible suggestion for the mechanism of elongation arrest is based on the conformational requirements of the Pro in the active site, as well as the bulky residues Trp and perhaps also Ile within the tunnel. By modeling a polyalanine nascent chain in the exit tunnel, we verified that once the proline has been incorporated into the nascent chain with the abovementioned sequence — that is, it is placed at the tunnel entrance — the two bulky residues Trp and Ile residues reach the tip of L22 β-hairpin (Fig. 3). The restricted conformational space of Pro may require a conformation of the nascent chain that leads Trp and Ile to trigger a swing in the L22 β-hairpin, in a manner similar to the action of TAO. This motion will free space for the bulky side chains but, at the same time, will jam the tunnel for the progression of bulky nascent chains, although it provides barely sufficient space for the progression of sequences with smaller side chains.

Consistent with our suggested mechanism is the finding that both the position of Trp and the spacing between Pro and Trp are crucial for elongation arrest of the nascent leader peptide of *E. coli* tryptophanase (tnaC) operon[8]. Also, our proposal is in line with the known ribosomal arrest-suppressing mutations of L22 (ref. 7). The alterations in *E. coli* L22 (G91S, A93T and A93V) introduce bulkier residues that, in the presence of the nascent chain, may destabilize the swung conformation. Furthermore, to better understand the arrest-alleviation induced by the deletion of Met82EC-Lys-Arg in L22 (ref. 7), which are also known to confer erythromycin resistance, we superposed the recently reported structure of this mutant (PDB entry 1I4J)[25] onto L22 in D50S structure. We observed that this deletion shortens the L22 β-hairpin and displaces the hinge region, compared with its position in native D50S. This displacement should not seriously affect the extensive interactions of L22 hairpin with the tunnel wall in the native structure, whereas it may alter the swing motion. Consequently the flipping of the tip of L22 β-hairpin may be hampered or performed in a way that prevents the formation of the stabilizing interactions with the opposite side of the tunnel. As observed[23], this deletion should affect the conformation of the nucleotides participating in erythromycin binding, confirming our proposal that erythromycin resistance is due to indirect effects[13]. Importantly, all known arrest suppression mutations of rRNA, such as the insertion of an adenine in the region A749EC–A753EC and the A2058EC mutation, occur close to the L22 β-hairpin, thus possibly affecting its conformation.

Under normal conditions, the SecM elongation arrest was found to be transient. However, in the absence of active export of SecM, the arrest is significantly prolonged[7]. Still to be investigated is the mechanism whereby the cellular signaling for alleviating the arrest is transmitted. A conformational change of the swung region that allows sufficient space for the progression of the nascent protein may be triggered through L22 β-strand extension of the hairpin, which extends all the way to its C terminus and, in the ribosome, is located at the vicinity of the exit-tunnel opening[12], thus possibly interacting with the 'pulling protein'. We also note that structural changes of the translocon pore, which lines up directly with the exit tunnel, were shown to be affected by the nascent chains from inside the ribosome[26]. In contrast, the nascent chain itself may also play a role in the suppression of the elongation arrest because, when the ribosome is stalled, the export signaling sequence of SecM[9] has already emerged out of the exit tunnel and may interact with the 'pulling protein'.

## Conclusions

The crystal structure of D50S in complex with TAO adds new insights into the mechanisms of action of macrolides. It indicates that macrolide drugs can hamper the progression of nascent chains by binding in various modes and shows the first case of an antibiotic blocking the tunnel by inducing conformational alterations in a ribosomal protein. Our results show that the L22 protein has an intrinsic conformational mobility and that its conserved double-hook feature, capable of interacting with two sides of the tunnel wall, creates a swinging gate within

**Table 1 Crystallographic data**

| | |
|---|---|
| Space group | *I*222 |
| Wavelength (Å) | 1.038 |
| Unit cell parameters (Å) | |
| *a* | 170.3 |
| *b* | 411.1 |
| *c* | 695.5 |
| Resolution range (Å) | 20–3.4 |
| Mosaicity (°) | 0.3 |
| Number of unique reflections | 291,247 |
| Completeness (%)[1] | 88.1 (84.5) |
| $R_{merge}$ (%)[1] | 9.9 (43.2) |
| $\langle I \rangle / \langle \sigma (I) \rangle$[1] | 5.4 (1.4) |
| Redundancy[1] | 2.4 (2) |
| *R*-factor (%) | 26.2 |
| $R_{free}$ (%)[2] | 31.0 |
| R.m.s. deviations from ideality | |
| Bond lengths (Å) | 0.0073 |
| Bond angles (°) | 1.31 |

[1]Values in parentheses refer to the highest resolution shell (3.46–3.4 Å).
[2]Calculated for a test reflection set (5% of the total) which was excluded from the refinement.

the tunnel that may control the nascent chain elongation. This outstanding role of L22 and the conservation of its β-hairpin size and sequence suggest the discriminating mechanism to be universal. Altogether, the observed ability of the ribosomal tunnel to oscillate between conformations, the known sequence dependence of the elongation arrest and the existence of arrest-suppression mutations that may affect the L22 conformation indicate that the tunnel is involved in sequence discrimination and plays an active role in regulation of intracellular processes.

## Methods

**TAO-resistant mutations.** Resistant mutants were induced by growing several generations in the presence of increasing concentrations of TAO (T.A., D.B. and A.Y., to be published).

**RNA probing.** RNA nucleotides were probed by footprinting protection of dimethyl sulfate (DMS) reaction as described[27].

**Crystallization and data collection.** Crystals of D50S[11] were soaked in solutions containing 0.1 mM TAO (Sigma). Data were collected at 100 K at ID29/ESRF/EMBL and ID19/APS/ANL, using Quantuum-210 and APS detectors, respectively. Data were processed with DENZO/SCALEPACK[28], HKL2000 (ref. 28) and the CCP4 suite[29] (Table 1).

**Structure refinement and modeling.** Overall and group rigid body refinements were performed with CNS[30] using the 3.0 Å resolution structure of D50S (PDB entry 1LNR) as a starting model. A substantial improvement of the Fourier electron density ($F_o - F_c$) and ($2F_o - F_c$) maps was achieved by solvent flattening using SOLOMON[29]. Two major peaks of positive density were identified in the maps in the region of the exit tunnel. TAO was placed unambiguously in one of them. The second positive density region deeper in the tunnel, together with a negative density peak at the location of the tip of the native L22 β-hairpin, was clearly interpreted as a novel conformation of the β-hairpin (Fig. 2). TAO, the L22 β-hairpin and the nascent chain were modeled using O[31]. Further refinement was carried out using CNS[30]. The nascent polypeptide chain, kinked to comply with the curvature of the tunnel, was modeled with an extended *trans* conformation and minimized in CNS.

Hinge regions for the L22 β-hairpin motion from the native to the swung conformation were identified by calculating Cα-based torsion angles[32] variations. Figures were produced with RIBBONS[33] and LigPlot[34].

**Coordinates.** The coordinates have been deposited in the protein data bank (accession code 1OND).


### Acknowledgments

We thank G. Glaser, R. Zarivach and P. Fucini for critical discussions; I. Agmon, R. Albrecht, C. Liebe, A. Wolff, H. Bartels, W.S. Bennett, E. Ben-Zeev, C. Glotz, H.A.S. Hansen, M. Kessler and A. McLeod for participating in this work; and the staff at ID19/SBC/APS and ID29/ESRF/EMBL. The Max-Planck-Society, the US National Institutes of Health, the German Science & Technology Ministry and the Kimmelman Center for Macromolecular Assembly provided support. A.Y. holds the Hellen and Martin Kimmel Professorial Chair.

### Competing interests statement

The authors declare that they have no competing financial interests.

Received 3 September, 2002; accepted 6 March, 2003.



1. Milligan, R.A. & Unwin, P.N. Location of exit channel for nascent protein in 80S ribosome. *Nature* **319**, 693–695 (1986).
2. Yonath, A., Leonard, K.R. & Wittmann, H.G. A tunnel in the large ribosomal subunit revealed by three-dimensional image reconstruction. *Science* **236**, 813–816 (1987).
3. Gabashvili, I.S. *et al*. The polypeptide tunnel system in the ribosome and its gating in erythromycin resistant mutants of L4 and L22. *Mol. Cell* **8**, 181–188 (2001).
4. Tenson, T. & Ehrenberg, M. Regulatory nascent peptides in the ribosomal tunnel. *Cell* **108**, 591–594 (2002).
5. Morris, D.R. & Geballe, A.P. Upstream open reading frames as regulators of mRNA translation. *Mol. Cell. Biol.* **20**, 8635–8642 (2000).
6. Sarker, S., Rudd, K.E. & Oliver, D. Revised translation start site for *secM* defines an atypical signal peptide that regulates *E. coli secA* expression. *J. Bacteriol.* **182**, 5592–5595 (2000).
7. Nakatogawa, H. & Ito, K. The ribosomal exit tunnel functions as a discriminating gate. *Cell* **108**, 629–636 (2002).
8. Gong, F. & Yanofsky, C. Instruction of translating ribosome by nascent peptide. *Science* **297**, 1864–1867 (2002).
9. Stroud, R.M. & Walter, P. Signal sequence recognition and protein targeting. *Curr. Opin. Struct. Biol.* **9**, 754–759 (1999).
10. Nissen, P., Hansen, J., Ban, N., Moore, P.B. & Steitz, T.A. The structural basis of ribosome activity in peptide bond synthesis. *Science* **289**, 920–930 (2000).
11. Harms, J. *et al*. High resolution structure of the large ribosomal subunit from a mesophilic eubacterium. *Cell* **107**, 679–688 (2001).
12. Unge, J. *et al*. The crystal structure of ribosomal protein L22 from *Thermus thermophilus*: insights into the mechanism of erythromycin resistance. *Structure* **6**, 1577–1586 (1998).
13. Schluenzen, F. *et al*. Structural basis for the interaction of antibiotics with the peptidyl transferase centre in eubacteria. *Nature* **413**, 814–821 (2001).
14. Hansen, J.L. *et al*. The structures of four macrolide antibiotics bound to the large ribosomal subunit. *Mol. Cell* **10**, 117–128 (2002).
15. Schluenzen, F. *et al*. Structural basis for the antibiotic activity of ketolides and azalides. *Structure* **11**, 329–338 (2003).
16. Periti, P., Tonelli, F., Mazzei, T. & Ficari, F. Antimicrobial chemoimmunoprophylaxis in colorectal surgery with cefotetan and thymostimulin: prospective, controlled multicenter study. Italian Study Group on Antimicrobial Prophylaxis in Abdominal Surgery. *J. Chemother.* **5**, 37–42 (1993).
17. Chepkwony, H.K., Roets, E. & Hoogmartens, J. Liquid chromatography of troleandomycin. *J. Chromatogr. A* **914**, 53–58 (2001).
18. Tenson, T. & Mankin, A.S. Short peptides conferring resistance to macrolide antibiotics. *Peptides* **22**, 1661–1668 (2001).
19. Verdier, L., Gharbi-Benarous, J., Bertho, G., Mauvais, P. & Girault, J.P. Antibiotic resistance peptides: interaction of peptides conferring macrolide and ketolide resistance with *Staphylococcus aureus* ribosomes: conformation of bound peptides as determined by transferred NOE experiments. *Biochemistry* **41**, 4218–4229 (2002).
20. Douthwaite, S., Hansen, L.H. & Mauvais, P. Macrolide-ketolide inhibition of MLS-resistant ribosomes is improved by alternative drug interaction with domain II of 23S rRNA. *Mol. Microbiol.* **36**, 183–193 (2000).
21. Weisblum, B. Erythromycin resistance by ribosome modification. *Antimicrob. Agents Chemother.* **39**, 577–585 (1995).
22. Hansen, L.H., Mauvais, P. & Douthwaite, S. The macrolide-ketolide antibiotic binding site is formed by structures in domains II and V of 23S ribosomal RNA. *Mol. Microbiol.* **31**, 623–631 (1999).
23. Xiong, L., Shah, S., Mauvais, P. & Mankin, A.S. A ketolide resistance mutation in domain II of 23S rRNA reveals the proximity of hairpin 35 to the peptidyl transferase centre. *Mol. Microbiol.* **31**, 633–639 (1999).
24. Goldman, R.C., Fesik, S.W. & Doran, C.C. Role of protonated and neutral forms of macrolides in binding to ribosomes from Gram-positive and Gram-negative bacteria. *Antimicrob. Agents Chemother.* **34**, 426–431 (1990).
25. Davydova, N., Streltsov, V., Wilce, M., Liljas, A. & Garber, M. L22 ribosomal protein and effect of its mutation on ribosome resistance to erythromycin. *J. Mol. Biol.* **322**, 635–644 (2002).
26. Liao, S., Lin, J., Do, H. & Johnson, A.E. Both lumenal and cytosolic gating of the aqueous ER translocon pore are regulated from inside the ribosome during membrane protein integration. *Cell* **90**, 31–41 (1997).
27. Stern, S., Moazed, D. & Noller, H.F. Structural analysis of RNA using chemical and enzymatic probing monitored by primer extension. *Methods Enzymol.* **164**, 481–489 (1988).
28. Otwinowski, Z. & Minor, W. Processing of X-ray diffraction data collected in oscillation mode. *Methods Enzymol.* **276**, 307–326 (1997).
29. Bailey, S. The CCP4 suite — programs for protein crystallography. *Acta Crystallogr. D* **50**, 760–763 (1994).
30. Brunger, A.T. *et al*. Crystallography & NMR system: a new software suite for macromolecular structure determination. *Acta Crystallogr. D* **54**, 905–921 (1998).
31. Jones, T.A., Zou, J.Y., Cowan, S.W. & Kjeldgaard, M. Improved methods for building protein models in electron density maps and the location of errors in these models. *Acta Crystallogr. A* **47**, 110–119 (1991).
32. Flocco, M.M. & Mowbray, S.L. Cα-based torsion angles: a simple tool to analyze protein conformational changes. *Protein Sci.* **4**, 2118–2122 (1995).
33. Carson, M. Ribbons. *Methods Enzymol.* **277**, 493–505 (1997).
34. Wallace, A.C., Laskowski, R.A. & Thornton, J.M. LIGPLOT: a program to generate schematic diagrams of protein-ligand interactions. *Protein Eng.* **8**, 127–134 (1995).